

# Electron transport under an ultrafast laser pulse: Implication for spin transport

Robert Meadows<sup>a</sup>, Y. Xue<sup>b</sup>, Nicholas Allbritton<sup>a</sup>, and G. P. Zhang<sup>a\*</sup>

<sup>a</sup>*Department of Physics, Indiana State University, Terre Haute, IN 47809, USA and*

<sup>b</sup>*Milwaukee Area Technical College, Milwaukee, WI 53233-1443*

(Dated: October 23, 2023)

## Abstract

Laser-driven electron transport across a sample has garnered enormous attentions over several decades, because it potentially allows one to control spin transports in spintronics. But light is a transverse electromagnetic wave, how an electron acquires a longitudinal velocity has been very puzzling. In this paper, we show a general mechanism is working. It is the magnetic field  $\mathbf{B}$  that steers the electron moving along the light propagation direction, while its strong transverse motion leads to local excitation. We employ the formalism put forth by Varga and Török to show that if we only include  $\mathbf{E}$ , the electron only moves transversely with a large velocity. Including both  $\mathbf{B}$  and  $\mathbf{E}$  and using real experimental laser parameters, we are able to demonstrate that a laser pulse can drive the electron along the axial direction by 20 to 262 Å, consistent with the experiments. The key insight is that  $\mathbf{B}$  changes the direction of the electron and allows the electron to move along the Poynting vector of light. Our finding has an important consequence. Because a nonzero  $\mathbf{B}$  means a spatially dependent vector potential  $\mathbf{A}(\mathbf{r}, t)$ ,  $\mathbf{B} = \nabla \times \mathbf{A}(\mathbf{r}, t)$ , this points out that the Coulomb gauge, that is, replacing  $\mathbf{A}(\mathbf{r}, t)$  by a spatial independent  $\mathbf{A}(t)$ , is unable to describe electron and spin transport under laser excitation. Our finding is expected to have a potential impact on the ongoing investigation of laser-driven spin transport.

Laser-induced electron and spin transport has attracted a broad attention over several decades [1–11]. In 1987, using an ultrashort laser pulse, Brorson *et al.* [1] showed that the heat transport is very rapid across the Au film, with the velocity close to the Fermi velocity. Aeschlimann *et al.* [12] estimated that the excited electron velocity is  $2 \times 10^8$  cm/s and the inelastic mean free path of 400 Å in Au. In 2011, Melnikov *et al.* [13] detected laser-excited spin-polarized carriers in Au/Fe/MgO(001). Transient spin current from ultrafast demagnetization in a ferromagnetic Co/Pt layer can create a measurable spin accumulation in Cu, Ag and Au [14]. Huisman *et al.* [15], using THz emission spectroscopy, detected spin currents in GdFeCo. The temporal profile of spin pulses indicates ballistic transport of hot electrons across the spin valves [16]. Thermovoltages and tunneling magneto-Seebeck ratio sensitively depend on the laser spot diameter [17]. Even the exchange bias can be changed [18]. Hot electrons alone can demagnetize a sample [19]. Theoretically, Lugovskoy and Bray [20] employed a Volkov wavefunction to investigate electron dynamics. Several studies adopted a time-dependent temperature in the Fermi distribution [21, 22], while others were based on the spin superdiffusion transport [23–25], but this is proved to be controversial [26, 27]. Moisan *et al.* [28] found that hot electron spin dependent transfer between neighboring domains does not alter ultrafast demagnetization. Including a laser field is possible in the Boltzmann equation, where nonequilibrium electron distribution can be treated [29–31]. In the atomistic spin simulation [32], Vahaplar *et al.* [33] introduced a phenomenological optomagnetic field. Fognini *et al.* [34] adopted a thermodynamic approach to ultrafast spin current, where laser pumping effect is encoded in the electron population change. Shokeen *et al.* [35] contrasted spin flips and spin transport processes and found that spin flip dominates in Ni but in Co both play a role. This result is consistent with the experiment in Ni, where Schellekens *et al.* [36] were unable to detect any major differences in Ni thin films on conducting and insulating substrates. An excellent review on hot-electron transport and demagnetization was given by Malinowski *et al.* [37]. So the central question [38, 39] is why and how the electron could gain the longitudinal velocity.

The goal of this paper is to investigate how a single laser pulse could drive the electron in a thin film down the axial direction so fast and so long. We employ Varga and Török’s method, which is based on the Hertz vector and satisfies the Maxwell equation, to carry out a series of simulations. We find a general conclusion. While the electron oscillates strongly along the transversal direction and moves very little, its axial velocity does not oscillate and

is unidirectional along the light propagation direction. Using an IR pulse of 1.6 eV moves the electron along the axial direction by  $z = 20\text{\AA}$ .  $z$  quadratically depends on the laser field amplitude and linearly depends on the pulse duration. When we reduce the photon energy  $\hbar\omega$  to 0.1 eV,  $z$  can reach over 120  $\text{\AA}$ , Reducing  $\hbar\omega$  to 0.06 eV,  $z$  reaches 262  $\text{\AA}$  even with a weak pulse of  $0.05\text{V}/\text{\AA}$ , which is now closer to the experimental observations [1, 13]. Assuming two different masses and two spin wavepacket spatial widths for majority and minority spins, our model can describe the spin moment change observed in experiments [40], without assuming spin superdiffusion. Central to our success is that although  $\mathbf{B}$  is much weaker than  $\mathbf{E}$ ,  $\mathbf{B}$  is the only one that can change the direction of electron motion, a result that might be not surprising to those in axial optics and plasma physics, but has been unknown in laser-induced electron transport community. This welcoming result requires a nonzero  $\mathbf{B}$ , but a nonzero  $\mathbf{B}$  subsequently requires a spatially dependent vector potential  $\mathbf{A}(\mathbf{r}, t)$ , owing to  $\mathbf{B} = \nabla \times \mathbf{A}(\mathbf{r}, t)$ . This has an important ramification. The dipole approximation is frequently employed in model and first-principles theories [41–44], but in order to describe electron transports in thin films, one has to use  $\mathbf{A}(\mathbf{r}, t)$ , not  $\mathbf{A}(t)$ . Our finding will have an important impact on future ultrafast electron and spin transport [1, 13, 45–47].

A fundamental difference between the electric-field-induced transport and laser-induced transport is that the latter does not have a voltage bias along the carrier moving direction. A light wave propagating toward a sample along the  $z$  axis has its electric-field  $\mathbf{E}$  along the  $x$  axis and the magnetic field  $\mathbf{B}$  along the  $y$  axis. Figure 1 schematically illustrates a typical experimental geometry.

The Hamiltonian of the electron inside an electromagnetic field is

$$H = \frac{1}{2m_e}(\mathbf{p} - q\mathbf{A}(\mathbf{r}, t))^2 + q\phi, \quad (1)$$

where  $\mathbf{A}(\mathbf{r}, t)$  is the vector potential,  $\phi$  is the scalar potential,  $q$  is the charge of the electron, and  $\mathbf{p}$  is the electron momentum. The equation of motion is given in terms of the generalized Lorentz force as [48],

$$m\frac{d^2\mathbf{r}}{dt^2} = q\mathbf{E}(\mathbf{r}, t) + \frac{q}{2m}(\mathbf{p} \times \mathbf{B}(\mathbf{r}, t) - \mathbf{B}(\mathbf{r}, t) \times \mathbf{p}) - \frac{q^2}{m}(\mathbf{A}(\mathbf{r}, t) \times \mathbf{B}(\mathbf{r}, t)). \quad (2)$$

If we set  $\mathbf{B}(\mathbf{r}, t)$  to zero, then every term, except the first term, on the right side, is zero, so the electron only moves along  $\mathbf{E}(\mathbf{r}, t)$ . This demonstrates that it is indispensable to include

$\mathbf{B}(\mathbf{r}, t)$ . In the limit that  $\mathbf{B}$ , not  $\mathbf{A}(\mathbf{r}, t)$ , is independent of space, one recovers the usual Lorentz force,

$$m \frac{d^2 \mathbf{r}}{dt^2} = q \mathbf{E} + q \mathbf{v} \times \mathbf{B}, \quad (3)$$

where the velocity  $\mathbf{v}$  is defined through the mechanical momentum  $\mathbf{v} \equiv \frac{\mathbf{p} - q \mathbf{A}(\mathbf{r}, t)}{m}$ .

We follow Varga and Török [49], and start from the Hertz vector, which satisfies the vectorial Helmholtz equation, so the resultant electric and magnetic fields automatically satisfy the Maxwell equation, given in an integral form as

$$\mathbf{E} = \frac{1}{2\pi k^2} \int_{-\infty}^{\infty} \int_{-\infty}^{\infty} \mathbf{g}(k_x, k_y) F(k_x, k_y) e^{i(k_x x + k_y y + k_z z)} dk_x dk_y, \quad (4)$$

and the magnetic field is

$$\mathbf{B} = -\frac{i\sqrt{\epsilon\mu}}{2\pi k} \int_{-\infty}^{\infty} \int_{-\infty}^{\infty} \mathbf{m}(k_x, k_y) F(k_x, k_y) e^{i(k_x x + k_y y + k_z z)} dk_x dk_y, \quad (5)$$

where  $\mathbf{g}(k_x, k_y) = (k^2 - k_x^2)\hat{x} - k_x k_y \hat{y} - k_x k_z \hat{z}$ ,  $\mathbf{m}(k_x, k_y) = k_z \hat{y} - k_y \hat{z}$ , and  $F$  is given by

$$F(k_x, k_y) = \frac{1}{2\pi} \int_{-\infty}^{\infty} \int_{-\infty}^{\infty} V(x, y, 0) e^{-i(k_x x + k_y y)} dx dy.$$

Here  $V(x, y, 0) = A_0 e^{-\frac{(x^2 + y^2)}{w_0^2}}$  has the dimension of the electric field, where  $A_0$  is the field amplitude and  $w_0$  is the pulse spatial width chosen as  $10\lambda$ .  $\lambda$  is the wavelength of the pulse.

Within the paraxial approximation, we integrate the above equations analytically to get the reduced  $\tilde{\mathbf{E}}$  and  $\tilde{\mathbf{B}}$ ,

$$\begin{aligned} \tilde{E}_x &= \left[ 1 + \frac{4x^2 - 2w_0^2}{w_0^4 k^2} \right], & \tilde{E}_y &= \frac{4xy}{w_0^4 k^2}, & \tilde{E}_z &= -\frac{2ik_z x}{w_0^2 k^2}. \\ \tilde{B}_x &= 0, & \tilde{B}_y &= -\frac{ik_z \sqrt{\epsilon\mu}}{k}, & \tilde{B}_z &= -\frac{2y \sqrt{\epsilon\mu}}{kw_0^2}. \end{aligned} \quad (6)$$

The final electric field and magnetic fields are

$$\mathbf{E} = A_0 \tilde{\mathbf{E}} e^{ik_z z - i\omega t - \left(\frac{x^2 + y^2}{w_0^2}\right)}, \quad \mathbf{B} = A_0 \tilde{\mathbf{B}} e^{ik_z z - i\omega t - \left(\frac{x^2 + y^2}{w_0^2}\right)}. \quad (7)$$

When the light enters a sample, both fields are reduced by  $e^{-z/(2\lambda_{pen})}$ , where  $\lambda_{pen}$  is the penetration depth and 2 comes from the fact that penetration depth is defined at  $1/e$  the incident fluence and the fluence is proportional to the square of the electric field.  $\lambda_{pen}$  is chosen to be 14 or 28 nm, typically values in fcc Ni.

In our study, we choose a linearly  $x$ -polarized pulse that is propagating along the  $z$  axis. The pulse is a Gaussian of duration  $\tau$ , amplitude  $A_0$  and photon energy  $\hbar\omega$ .  $A_0 e^{-i\omega t}$  in  $\mathbf{E}$

and  $\mathbf{B}$  in Eq. 7 is replaced by  $A_0 e^{-t^2/\tau^2} \cos(\omega t)$ , so our electric and magnetic fields are

$$\mathbf{E}(\mathbf{r}, t) = A_0 e^{-t^2/\tau^2} \cos(\omega t) \tilde{\mathbf{E}} e^{ik_z z - \frac{z}{2\lambda_{pe} n} - \left(\frac{x^2 + y^2}{w_0^2}\right)}, \quad (8)$$

$$\mathbf{B}(\mathbf{r}, t) = A_0 e^{-t^2/\tau^2} \cos(\omega t) \tilde{\mathbf{B}} e^{ik_z z - \frac{z}{2\lambda_{pe} n} - \left(\frac{x^2 + y^2}{w_0^2}\right)}. \quad (9)$$

These analytic forms of  $\mathbf{E}$  and  $\mathbf{B}$ , which contain both the spatial and temporal dependences, greatly ease our calculation. As a first step toward a complete transport theory, we treat the electron classically, and solve the Newtonian equation of motion numerically,

$$\frac{d\mathbf{v}}{dt} = \frac{q}{m} [\mathbf{E}(\mathbf{r}, t) + \mathbf{v} \times \mathbf{B}(\mathbf{r}, t)] - \frac{\mathbf{v}}{\Gamma}, \quad (10)$$

where  $m$  and  $q$  are the electron mass and charge respectively,  $\mathbf{v}$  is its velocity, and  $\Gamma$  is a small damping to mimick the resistance due to collision with other electrons and nuclei. Although our method is classical, it fully embraces the real space approach that is more suitable for transport, a key feature that none of prior first-principles and model simulations is able to achieve. This will answer the most critical question whether the electron can move along the axial direction.

We choose a pulse of  $\hbar\omega = 1.6$  eV,  $\tau = 180$  fs,  $A_0 = 0.15$  V/Å, often used in experiments [50]. We set the initial position and velocity of the electron to zero and  $\Gamma = 200$  fs. Figure 2(a) shows that the velocity along the  $x$  axis,  $v_x$ , increases very rapidly, with the maximum velocity reaching 1Å/fs,  $10^5$ m/s, on the same order of magnitude of the velocity found in Cu/Pt multilayers [51]. Unfortunately, the experimental fluence was not given, so a quantitative comparison is not possible. Nevertheless, this velocity also agrees with another experiment in Co/Cu(001) films [52]. Prior studies [23] often use the Fermi velocity to discuss spin transport, which is not appropriate. Instead, one must obtain the actual electron velocity first from the laser field, because in the absence of a laser field, the sum of the velocities among the electrons must be zero and there should be no transport. Although  $v_x$  has a peak value, it oscillates very strongly. By contrast, Fig. 2(b) shows the velocity  $v_z$  increases with time, without oscillation.  $v_z$  is always positive, increases smoothly and peaks around 100 fs. This peak time is set by the laser parameter and the damping  $\Gamma$ . Using a larger  $\Gamma$  leads to a larger  $v_z$ . The positivity of  $v_z$ , regardless of the type of charge, is crucial to the electron transport, and can be understood from the directions of  $\mathbf{E}$  and  $\mathbf{B}$ . Suppose at one instant of time,  $\mathbf{E}$  is along the  $+x$  axis and  $\mathbf{B}$  along the  $+y$  axis. The electron experiences a negative force along the  $-x$  axis and gains the velocity along the  $-x$  axis, so

the Lorentz force due to  $\mathbf{B}$  is along the  $+z$  direction. Now suppose at another instance,  $\mathbf{E}$  changes to  $-x$  and  $\mathbf{B}$  to  $-y$ , so the electron velocity is along  $+x$ , but the Lorentz force is still along the  $+z$  axis. If we have a positive charge, the situation is similar. The fundamental reason why we always have a positive force is because the light propagates along the  $+z$  axis and the Poynting vector is always along  $+z$  and  $\mathbf{v} \times \mathbf{B}$  points along the  $+z$  axis. We test it with various laser parameters and never find a negative  $v_z$ . Under cw approximation, Rothman and Boughn [53] gave a simple but approximate expression for the dimensionless  $v_z = \frac{1}{2} \left(\frac{\omega_c}{\omega}\right)^2 [\cos(\omega t) - 1]^2$ , and Hagenbuch [54] gave  $p_z = e^2 A^2(\tau')/2mc$ , both of which are positive. Therefore, both their theories and our numerical results with a pulse laser agree that the axial motion of the electron is delivered by both  $\mathbf{E}$  and  $\mathbf{B}$ . This is also consistent with the radiation pressure from a laser beam can accelerate and trap particles [55, 56].

Figure 2(c) shows the displacement along the  $x$  (solid line) and  $z$  (dashed line) axes, respectively. We see that  $x$  does not change very much. This shows that the electron excitation along the  $x$  axis is local. If we include the band structure of a solid, it will stimulate both intraband and interband transitions [57] and demagnetize the sample locally. In our simple classical model, these features cannot be included. But our study confirms the local heating must occur. Besides the direct demagnetization due to heating, it may stimulate magnon generation to destroy the magnetic long-range ordering [58]. Central to our research is whether the electron indeed moves along the axial direction. Figure 2(c) demonstrates clearly that the electron successfully moves along the  $z$  axis by 20 Å.

We can move one step further. Keeping the rest of laser parameters unchanged, we change the laser field amplitude  $A_0$  from 0.01 to 0.20 V/Å and then compute  $z$  for each amplitude. Figure 3(a) is our result. First we notice that  $z$  change is highly nonlinear. We fit it to a quadratic function,  $z = \alpha A_0^2$ , up to  $A_0 = 0.15\text{V}/\text{Å}$ , where  $\alpha = 919.254\text{Å}^3/\text{V}^2$ , and find that the fit is almost perfect. Because  $|A_0|^2$  is directly proportional to the fluence, this demonstrates  $z$  is linearly proportional to the laser fluence, which is exactly expected from the Poynting vector  $\mathbf{S} = \mathbf{E} \times \mathbf{B}/c$ . Thus, both qualitatively and quantitatively our results can be understood. What is less known is the dependence of  $z$  on laser pulse duration  $\tau$ . We change  $\tau$  from 60 to 180 fs. Figure 3(b) shows  $z$  increases with  $\tau$  linearly. As expected, the increase is steeper at 0.15V/Å (the circles) than that  $A_0 = 0.10\text{V}/\text{Å}$  (boxes). The duration dependence leads us to wonder whether the photon energy  $\hbar\omega$  also affects the axial motion of the electron.

We compute  $z$  with our photon energy going from 0.02 up to 1.6 eV, while keeping both the duration  $\tau = 180$  fs and amplitude  $A_0 = 0.05\text{V}/\text{\AA}$  fixed. Figure 3(c) shows an astonishing result:  $z$  is inversely proportional to  $\hbar\omega$ . At the lower end of  $\hbar\omega$ ,  $z$  exceeds 100  $\text{\AA}$ . Note that at such a low amplitude, a pulse of 1.6 eV only drives the electron by 2-3  $\text{\AA}$ . This explains why THz pulses become a new frontier for ultrafast demagnetization [59–61]. Polley *et al.* [62] employed a THz pulse to demagnetize CoPt films with a goal toward ultrafast ballistic switching. Shalaby *et al.* [63] showed that extreme THz fields with fluence above 100 mJ/cm<sup>2</sup> can induce a significant magnetization dynamics in Co, with the magnetic field becoming more important.

Our result uncovers an important picture. When the pulse oscillates more slowly, the electron gains more grounds. Of course, a DC current can move electrons even further, but then it does not have enough field intensity. This result can be tested experimentally.

We would like to see what happens to the electron under a THz pulse excitation. We choose a pulse of  $\hbar\omega = 0.06$  eV,  $\tau = 180$  fs and  $A_0 = 0.05\text{V}/\text{\AA}$ . Figure 4(a) shows that  $v_z$  reaches 0.14  $\text{\AA}/\text{fs}$ , which is three times that with  $\hbar\omega = 1.6$  eV and  $A_0 = 0.15\text{V}/\text{\AA}$  in Fig. 2(b). Our laser pulse is shown in the inset of Fig. 4(a). We should mention that our current  $v_x$  has a peak value of around 10  $\text{\AA}/\text{fs}$ , close to the Fermi velocity as found in the experiments [1, 13]. Figure 4(b) shows that  $z$  reaches 55  $\text{\AA}$ . Increasing  $A_0$  to 0.15 V/ $\text{\AA}$  boosts  $v_z$  by four times (Fig. 4(c)) and increases  $z$  to 262  $\text{\AA}$ . This distance is closer to the experimental value. Melnikov *et al.* [13] employed a multilayer structure, (50 nm Au)/(15 nm Fe)/MgO(001). Once they increase the thickness of Au to 100 nm, they find a delay signal in second-harmonic generation. This shows the electron in Au can travel a much longer distance [64], suggesting that our  $\Gamma$  may be still too short. A much stronger effect is found in plasma [65]. This may indicate the free electron mass used in our study may be too big.

This opens the door to investigate the spin transport by using two different effective masses of the electron. Since the effective mass of the majority spin is always smaller than that of the minority spin, we assume  $m_\uparrow = m_e$  and  $m_\downarrow = 2m_e$ . Naturally, this huge difference is somewhat exaggerated, but our intention is to see whether this difference could produce something that can be related to experiments. With these different masses, we compute the  $z_\uparrow$  and  $z_\downarrow$  separately. We employ the same laser parameters as above:  $A_0 = 0.05\text{V}/\text{\AA}$ ,  $\hbar\omega = 0.06$  eV, and  $\tau = 180$  fs. For the same force, the acceleration  $a_\uparrow$  is larger than  $a_\downarrow$ ,

since  $a = F/m$ . Figure 5(a) shows  $z(t)$  for spin up and spin down. It is clear that  $z_\downarrow$  is smaller than  $z_\uparrow$ , as expected. This means that the majority spin electron moves away from the origin earlier.

The next question is how we can relate  $z$  to the spin. We recall that the classical position is always a good measure for the center of the wavepacket of the electron in quantum mechanics. In our mind, we envision that a wavepacket of some size is centered around  $z(t)$ . As time goes by, the center moves. Henn *et al.* [66] showed that the excited electron spin spreads as a spin packet. Since we do not know the width of the wavepacket, we introduce them as a parameter. We choose a simple one-dimensional Gaussian wavepacket, with the wavefunction  $\psi(z, t) = Ce^{-\beta z^2(t)}e^{ik_z z}$ , where  $\beta$  and  $C$  are constants. Other types should work as well. We take fcc Ni as our target example. The number of  $3d$  electrons in the spin majority channel is about 5, while that in the minority is 4.46. This leads to the spin moment of  $0.54 \mu_B$  [67]. The many-body density  $\rho = |\psi|^2$  is related to the electron number, and then we have the spin moment at location  $z = 0$  as

$$M_z(\mu_B)(t) = 5e^{-(z_\uparrow^2(t))/w_\uparrow^2} - 4.46e^{-(z_\downarrow^2(t))/w_\downarrow^2}, \quad (11)$$

where both  $z_\uparrow$  and  $z_\downarrow$  are referenced to  $z = 0$  and  $w_{\uparrow(\downarrow)}$  is the width of spin majority (minority) wavepacket. This equation has a nice feature. At  $t = 0$ ,  $M_z$  is  $0.54 \mu_B$ . As the electrons move away from  $z = 0$ , the local spin moment change sensitively depends on  $w_\uparrow$  and  $w_\downarrow$ . It turns out that we cannot arbitrarily choose them, because they immediately lead to an unphysical spin moment change. Too small values cannot reproduce experimental results. A positive  $M_z > 0$  means

$$e^{+(z_\uparrow^2(t))/w_\uparrow^2 - (z_\downarrow^2(t))/w_\downarrow^2} > 4.46/5 \rightarrow \frac{z_\uparrow^2}{w_\uparrow^2} - \frac{z_\downarrow^2}{w_\downarrow^2} < 0.1142. \quad (12)$$

For  $w_\uparrow = 100\text{\AA}$ ,  $w_\downarrow = 24.5\text{\AA}$ , Fig. 5(b) shows an increase in  $M_z$ , which is very similar to Fig. 2(a) of Ref. [40]. The reason is that when the majority wavepacket has a larger width, the majority spin dominates over the minority spin. Once we increase  $w_\downarrow$  to  $30\text{\AA}$ , we see there is a demagnetization, similar to Figs. 2(b), 2(c) and 2(d) of Ref. [40], without assuming spin superdiffusion. Increasing  $w_\downarrow$  further to  $70.7\text{\AA}$  flips the spin to the opposite direction, which resembles to all-optical spin switching [45]. Since the electron scattering and other scatterings are taken into account through  $\Gamma$ , our results are applicable to solids. Our finding reminds us the earlier study by von Korff Schmising *et al.* [68], where within a



few hundred fs magnetization reduction has a spatial distribution. In our picture, magnetic and electric fields of the laser pulse jointly drive the electron down along the axial direction as a wavepacket (see Fig. 1).

Our approach is in sharp contrast to the prior studies, where the axial motion is empirically included [23] or simulated by chemical potential [4, 7, 34]. Indeed, Ashok and coworkers [69] started with a space- and time-dependent transient chemical potential and computed the internal electric field from the chemical potential and then current using the Ohm's law. Hurst *et al.* [70] recognized the importance of the magnetic field and adopted the spin-Vlasov equation, instead of the Boltzmann equation. To simulate the external electric field effect, they shifted the distribution by a constant velocity  $\Delta v$ . Choi *et al.* [4, 14] gave the spin accumulation through the spin diffusion equation as

$$\frac{\partial \mu_s}{\partial t} = D \frac{\partial^2 \mu_s}{\partial z^2} - \frac{\mu_s}{\tau_s}, \quad (13)$$

where  $\mu_s = \mu_\uparrow - \mu_\downarrow$  is the spin chemical potential and  $D$  is the spin diffusion constant, and  $\tau_s$  is the spin relaxation time. This approach follows the electric-field induced transport, where a voltage bias is applied across a device and the chemical potential difference maintained between the drain and source drives the charge carrier across the device [71]. So the charge carriers move along the electric field. In a shorter channel, the transport can be ballistic, while in a longer channel, it is diffusive.

Our finding has several important implications. First, although the magnetic field is much weaker than the electric field, if we ignore it, the electron only moves along the  $x$  axis. Therefore, it is absolutely necessary to include the magnetic field, because it is the magnetic field that changes the direction of the electron motion [54]. This is also consistent with the Poynting vector, thus, the momentum, which is in the direction of light propagation. Although ignoring the magnetic field greatly eases numerical calculation, it cannot describe the laser-induced electron transport. Second, because  $\mathbf{B} = \nabla \times \mathbf{A}$ , where  $\mathbf{A}$  is the vector potential, not to be confused with the laser field amplitude  $A_0$ . A nonzero  $\mathbf{B}$  means that  $\mathbf{A}$  must contain  $\mathbf{r}$  as its variable. The regular dipole approximation,  $\mathbf{A}(\mathbf{r}, t) \rightarrow \mathbf{A}(t)$ , is not appropriate, if one wishes to describe the electron transport along the axial direction, but nearly all prior theoretical studies employ this approximation [23, 41–44]. For instance, the first model simulation [72] and even more recent first-principles investigations [41, 42, 44] used a vector potential  $\mathbf{A}$  that is independent of space. Such an approach, called the dipole

approximation, is reasonable if the wavelength of a laser pulse is much larger than the area illuminated and the focus is on the electronic excitation, rather than transport. Without a spatial dependence, the electron only moves along the  $\mathbf{E}$  field direction [73] which is transversal to the light propagation direction and the oscillating current is exactly in the same direction as the polarization [74].

In conclusion, we have shown that the electron transport under an ultrafast laser pulse is most likely due to the joint effect of the electric and magnetic fields. Each field alone cannot introduce the transport along the axial direction. The electric field provides a strong transversal velocity, while the magnetic field steers the electron moving along the light propagation direction. With the experimental accessible laser field parameters, we demonstrate that the electron can move up to 20 to 262 Å, which now agree with the prior experiments [1, 13]. Our finding points out a serious problem with the existing theories where the vector potential has no spatial dependence but is used to describe the transport. Our theory goes beyond the classical Boltzmann equation and chemical potential change, and puts the transport physics on a solid foundation. This potentially opens the door to more advanced first-principles theory, which has a significant impact on future technology in charge and spin transports [1, 13, 38, 39, 45–47, 75].

This work was partially supported by the U.S. Department of Energy under Contract No. DE-FG02-06ER46304. Part of the work was done on Indiana State University’s high performance Quantum and Obsidian clusters. The research used resources of the National Energy Research Scientific Computing Center, which is supported by the Office of Science of the U.S. Department of Energy under Contract No. DE-AC02-05CH11231.

\* guo-ping.zhang@outlook.com. <https://orcid.org/0000-0002-1792-2701>

The data that support the findings of this study are available from the corresponding author upon reasonable request.

- 
- [1] S. D. Brorson, J. G. Fujimoto, and E. P. Ippen, Femtosecond electronic heat-transport dynamics in thin gold films, *Phys. Rev. Lett.* **59**, 1962 (1987).
- [2] H.-G. Boyen, R. Gampp, P. Oelhafen, B. Heinz, P. Ziemann, Ch. Lauinger and St. Herminghaus, Intraband transitions in simple metals: Evidence for non-Drude-like near-IR optical

- properties, Phys. Rev. B **56**, 6502 (1997).
- [3] J. Hohlfeld, S.-S. Wellershoff, J. Güdde, U. Conrad, V. Jähnke and E. Matthias, Electron and lattice dynamics following optical excitation of metals, Chem. Phys. **251**, 237 (2000).
- [4] G.-M. Choi, B.-C. Min, K.-J. Lee and D. G. Cahill, Spin current generated by thermally driven ultrafast demagnetization, Nat. Comm. **5**, 4334 (2014).
- [5] B. Vodungbo, J. Gautier, G. Lambert, A. B. Sardinha, M. Lozano, S. Sebban, M. Ducouso, W. Boutu, K. Li, B. Tudu, M. Tortarolo, R. Hawaldar, R. Delaunay, V. Lopez-Flores, J. Arabski, C. Boeglin, H. Merdji, P. Zeitoun, and J. Lüning, Laser-induced ultrafast demagnetization in the presence of a nanoscale magnetic domain network, Nat. Commun. **3**, 999 (2012).
- [6] B. Pfau *et al.*, Ultrafast optical demagnetization manipulates nanoscale spin structure in domain walls, Nat. Commun. **3**, 1100 (2012).
- [7] J. Kimling and D. G. Cahill, Spin diffusion induced by pulsed-laser heating and the role of spin heat accumulation, Phys. Rev. B **95**, 014402 (2017).
- [8] M. Hofherr, P. Maldonado, O. Schmitt, M. Berritta, U. Bierbrauer, S. Sadashivaiah, A. J. Schellekens, B. Koopmans, D. Steil, M. Cinchetti, B. Stadtmüller, P. M. Oppeneer, S. Mathias, and M. Aeschlimann, Speed and efficiency of femtosecond spin current injection into a nonmagnetic material, Phys. Rev. B **96**, 100403(R) (2017).
- [9] T. Seifert, U. Martens, S. Günther, M. A. W. Schoen, F. Radu, X. Z. Chen, I. Lucas, R. Ramos, M. H. Aguirre, P. A. Algarabel, A. Anadon, H. S. Körner, J. Walowski, C. Back, M. R. Ibarra, L. Morellon, E. Saitoh, M. Wolf, C. Song, K. Uchida, M. Münzenberg, I. Radu and T. Kampfrath, SPIN **7**, 1740010 (2017).
- [10] T. S. Seifert, N. M. Tran, O. Gueckstock, S. M. Rouzegar, L. Nadvornik, S. Jaiswal, G. Jakob, V. V. Temnov, M. Münzenberg, M. Wolf, M. Kläui and T. Kampfrath, Terahertz spectroscopy for all-optical spintronic characterization of the spin-Hall-effect metals Pt, W and Cu<sub>80</sub>Ir<sub>20</sub>, J. Phys. D: Appl. Phys. **51**, 364003 (2018)
- [11] J. Chen *et al.*, Competing spin transfer and dissipation at Co/Cu(001) interfaces on femtosecond timescales, Phys. Rev. Lett. **122**, 067202 (2019).
- [12] M. Aeschlimann, M. Bauer and S. Pawlik, Chem. Phys. **205**, 127 (1996).
- [13] A. Melnikov, I. Razdolski, T. O. Wehling, E. Th. Papaioannou, V. Roddatis, P. Fumagalli, O. Aktsipetrov, A. I. Lichtenstein, and U. Bovensiepen, Ultrafast transport of laser-excited spin-polarized carriers in Au/Fe/MgO(001), Phys. Rev. Lett. **107**, 076601 (2011).

- [14] G.-M. Choi and D. G. Cahill, Kerr rotation in Cu, Ag, and Au driven by spin accumulation and spin-orbit coupling, *Phys. Rev. B* —bf 90, 214432 (2014).
- [15] T. J. Huisman and Th. Rasing, THz emission spectroscopy for THz spintronics, *J. Phys. Soc. Jpn.* **86**, 011009 (2017)
- [16] A. Alekhin, I. Razdolski, N. Ilin, J. P. Meyburg, D. Diesing, V. Roddatis, I. Rungger, M. Stamenova, S. Sanvito, U. Bovensiepen, and A. Melnikov, Femtosecond spin current pulses generated by the nonthermal spin-dependent Seebeck effect and interacting with ferromagnets in spin valves, *Phys. Rev. Lett.* **119**, 017202 (2017).
- [17] U. Martens, J. Walowski, T. Schumann, M. Mansurova, A. Boehnke, T. Huebner, G. Reiss, A. Thomas and M. Münzenberg, Pumping laser excited spins through MgO barriers, *J. Phys. D: Appl. Phys.* **50** 144003 (2017).
- [18] P. Vallobra, T. Fache, Y. Xu, L. Zhang, G. Malinowski, M. Hehn, J.-C. Rojas-Sanchez, E. Fullerton, and S. Mangin, Manipulating exchange bias using all-optical helicity-dependent switching, *Phys. Rev. B* **96**, 144403 (2017).
- [19] A. Eschenlohr, M. Battiato, P. Maldonado, N. Pontius, T. Kachel, K. Holldack, R. Mitzner, A. Föhlisch, P. M. Oppeneer, and C. Stamm, Ultrafast spin transport as key to femtosecond demagnetization, *Nat. Mater.* **12**, 332 (2013).
- [20] A. V. Lugovskoy and I. Bray, Ultrafast electron dynamics in metals under laser irradiation, *Phys. Rev. B* **60**, 3279 (1999).
- [21] E. Carpene, Ultrafast laser irradiation of metals: Beyond the two-temperature model, *Phys. Rev. B* **74**, 024301 (2006).
- [22] P. Kratzer, L. Rettig, I. Y. Sklyadneva, E. V. Chulkov and U. Bovensiepen, Relaxation of photo-excited hot carriers beyond multi-temperature models: A general theory description verified by experiments on Pb/Si(111), arXiv:2205.04958v1.
- [23] M. Battiato, K. Carva, and P. M. Oppeneer, Superdiffusive spin transport as a mechanism of ultrafast demagnetization, *Phys. Rev. Lett.* **105**, 027203 (2010).
- [24] D. Rudolf, C. La-O-Vorakiat, M. Battiato, R. Adam, J. M. Shaw, E. Turgut, P. Maldonado, S. Mathias, P. Grychtol, H. T. Nembach, T. J. Silva, M. Aeschlimann, H. C. Kapteyn, M. M. Murnane, C. M. Schneider, and P. M. Oppeneer, Ultrafast magnetization enhancement in metallic multilayers driven by superdiffusive spin current, *Nat. Commun.* **3**, 1037 (2012).
- [25] R. Gupta, F. Cosco, R. S. Malik, X. Chen, S. Saha, A. Ghosh, T. Pohlmann, J. R. L. Mardegan,

- S. Francoual, R. Stefanuik, J. Söderström, B. Sanyal, O. Karis, P. Svedlindh, P. M. Oppeneer, and R. Knut, Direct evidence of superdiffusive terahertz spin current arising from ultrafast demagnetization process, arXiv:2205.07974v1.
- [26] M. L. M. Laliou *et al.*, Deterministic all-optical switching of synthetic ferrimagnets using single femtosecond laser pulses, *Phys. Rev. B* **96**, 220411 (2017).
- [27] C. Stamm, C. Murer, M. S. Wörnle, Y. Acremann, R. Gort, S. Däter, A. H. Reid, D. J. Higley, S. F. Wandel, W. F. Schlotter and P. Gambardella, X-ray detection of ultrashort spin current pulses in synthetic antiferromagnets, *J. Appl. Phys.* **127**, 223902 (2020).
- [28] N. Moisan, G. Malinowski, J. Mauchain, M. Hehn, B. Vodungbo, J. Lüning, S. Mangin, E. E. Fullerton, and A. Thiaville, Investigating the role of superdiffusive currents in laser induced demagnetization of ferromagnets with nanoscale magnetic domains, *Sci. Rep.* **4**, 4658 (2014).
- [29] D. Bejan and G. Raseev, Nonequilibrium electron distribution in metals, *Phys. Rev. B* **55**, 4250 (1997).
- [30] N. Brouwer and B. Rethfeld, Excitation and relaxation dynamics in dielectrics irradiated by an intense ultrashort laser pulse, *J. Opt. Soc. Am. B* **31**, C28 (2014).
- [31] M. Beens, K. A. de Mare, R. A. Duine and B. Koopmans, Spin-polarized hot electron transport versus spin pumping mediated by local heating, arXiv:2208.14342v1.
- [32] R. F. L Evans, W. J. Fan, P. Chureemart, T. A. Ostler, M. O. A. Ellis and R. W. Chantrell, Atomistic spin model simulations of magnetic nanomaterials, *J. Phys. Condens. Matter* **26**, 103202 (2014).
- [33] K. Vahaplar, A. M. Kalashnikova, A. V. Kimel, S. Gerlach, D. Hinzke, U. Nowak, R. Chantrell, A. Tsukamoto, A. Itoh, A. Kirilyuk, and Th. Rasing, All-optical magnetization reversal by circularly polarized laser pulses: Experiment and multiscale modeling, *Phys. Rev. B* **85**, 104402 (2012).
- [34] A. Fognini, T. U. Michlmayr, A. Vaterlaus and Y. Acremann, Laser-induced ultrafast spin current pulses: a thermodynamic approach, *J. Phys.: Condens. Matter* **29**, 214002 (2017).
- [35] V. Shokeen, M. Sanchez Piaia, J.-Y. Bigot, T. Müller, P. Elliott, J. K. Dewhurst, S. Sharma, and E. K. U. Gross, Spin flips versus spin transport in nonthermal electrons excited by ultra-short optical pulses in transition metals, *Phys. Rev. Lett.* **119**, 107203 (2017).
- [36] A. J. Schellekens, W. Verhoeven, T. N. Vader, and B. Koopmans, Investigating the contribution of superdiffusive transport to ultrafast demagnetization of ferromagnetic thin films, *Appl.*

- Phys. Lett. **102**, 252408 (2013).
- [37] G. Malinowski, N. Berggaard, M. Hehn, and S. Mangin, Hot-electron transport and ultrafast magnetization dynamics in magnetic multilayers and nanostructures following femtosecond laser pulse excitation, *Eur. Phys. J. B* **91**, 98 (2018).
- [38] B. Liu, H. Xiao, and M. Weinelt, Microscopic insights to spin transport driven ultrafast magnetization dynamics in a Gd/Fe bilayer, *Sci. Adv.* **9**, eade0286(2023).
- [39] K. Kang, H. Omura, D. Yesudas, O. Lee, K.-J. Lee, H.-W. Lee, T. Taniyama, and G.-M. Choi, Spin current driven by ultrafast magnetization of FeRh, *Nat. Commun.* **14**, 3619 (2023).
- [40] E. Turgut, C. La-o-vorakiat, J. M. Shaw, P. Grychtol, H. T. Nembach, D. Rudolf, R. Adam, M. Aeschlimann, C. M. Schneider, T. J. Silva, M. M. Murnane, H. C. Kapteyn and S. Mathias, Controlling the competition between optically induced ultrafast spin-flip scattering and spin transport in magnetic multilayers, *Phys. Rev. Lett.* **110**, 197201 (2013).
- [41] G. P. Zhang, G. Lefkidis, W. Hübner, and Y. Bai, Ultrafast demagnetization in ferromagnets and magnetic switching in nanoclusters when the number of photons is kept fixed, *J. Appl. Phys.* **109**, 07D303 (2011).
- [42] K. Krieger, J. K. Dewhurst, P. Elliott, S. Sharma, and E. K. U. Gross, Laser-induced demagnetization at ultrashort time scales: Predictions of TDDFT, *J. Chem. Theory and Comput.* **11**, 4870 (2015).
- [43] Z. H. Chen and L. W. Wang, Role of initial magnetic disorder: A time-dependent ab initio study of ultrafast demagnetization mechanisms, *Sci. Adv.* **8**, eaau8000 (2019).
- [44] S. R. Acharya, V. Turkowski, G. P. Zhang, and T. Rahman, Ultrafast electron correlations and memory effects at work: Femtosecond demagnetization in Ni, *Phys. Rev. Lett.* **125**, 017202 (2020).
- [45] C. D. Stanciu, F. Hansteen, A. V. Kimel, A. Kirilyuk, A. Tsukamoto, A. Itoh, and Th. Rasing, All-optical magnetic recording with circularly polarized light, *Phys. Rev. Lett.* **99**, 047601 (2007).
- [46] G. P. Zhang, M. Murakami, M. S. Si, Y. H. Bai, and T. F. George, Understanding all-optical spin switching: Comparison between experiment and theory, *Mod. Phys. Lett. B* **32**, 1830003 (2018).
- [47] G. P. Zhang, R. Meadows, A. Tamayo, Y. H. Bai, and T. F. George, An attempt to simulate laser-induced all-optical spin switching in a crystalline ferrimagnet, *AIP Adv.* **10**, 125323

- (2020).
- [48] D. J. Griffiths and D. F. Schroeter, *Introduction to quantum mechanics*, Cambridge University Press, 3rd edition, page 182 (2018).
  - [49] P. Varga and P. Török, The Gaussian wave solution of Maxwell's equations and the validity of scalar wave approximation, *Opt. Commun.* **152**, 108 (1998).
  - [50] M. S. Si and G. P. Zhang, Resolving photon-shortage mystery in femtosecond magnetism, *J. Phys.: Condens. Matter* **22**, 076005 (2010).
  - [51] N. Berggaard, M. Hehn, S. Mangin, G. Lengaigne, F. Montaigne, M. L. M. Laliou, B. Koopmans, and G. Malinowski, Hot-electron-induced ultrafast demagnetization in Co/Pt multilayers, *Phys. Rev. Lett.* **117**, 147203 (2016).
  - [52] J. Wieczorek, A. Eschenlohr, B. Weidtmann, M. Rösner, N. Berggaard, A. Tarasevitch, T. O. Wehling, and U. Bovensiepen, Separation of ultrafast spin currents and spin-flip scattering in Co/Cu(001) driven by femtosecond laser excitation employing the complex magneto-optical Kerr effect, *Phys. Rev. B* **92**, 174410 (2015).
  - [53] T. Rothman and S. Boughn, The Lorentz force and the radiation pressure of light, *Am. J. Phys.* **77**, 122 (2009).
  - [54] K. Hagenbuch, Free electron motion in a plane electromagnetic wave, *Am. J. Phys.* **45**, 693 (1977).
  - [55] A. Ashkin, Acceleration and trapping of particles by radiation pressure, *Phys. Rev. Lett.* **24**, 156 (1970).
  - [56] A. Ashkin, J. M. Dziedzic, J. E. Bjorkholm, and S. Chu, Observation of a single-beam gradient force optical trap for dielectric particles, *Opt. Lett.* **11**, 288 (1986).
  - [57] M. Murakami and G. P. Zhang, Strong ultrafast demagnetization due to the intraband transitions, *J. Phys.: Condens. Matter* **35**, 495803 (2023).
  - [58] G. P. Zhang, M. Murakami, Y. H. Bai, T. F. George, and X. S. Wu, Spin-orbit torque-mediated spin-wave excitation as an alternative paradigm for femtomagnetism, *J. Appl. Phys.* **126**, 103906 (2019).
  - [59] M. Shalaby, C. Vicario, and C. P. Hauri, The terahertz frontier for ultrafast coherent magnetic switching: Terahertz-induced demagnetization of ferromagnets, [arxiv.org/abs/1506.05397](https://arxiv.org/abs/1506.05397).
  - [60] M. Hudl, M. d'Aquino, M. Pancald, S.-H. Yang, M. G. Samant, S. S. P. Parkin, H. A. Dürr, C. Serpico, M. C. Hoffmann, and S. Bonetti, Nonlinear Magnetization Dynamics Driven by



- Strong Terahertz Fields, Phys. Rev. Lett. **123**, 197204 (2019).
- [61] H. Lee, C. Weber, M. Fähnle and M. Shalaby, Ultrafast Electron Dynamics in Magnetic Thin Films, Appl. Sci. **11**, 9753 (2021).
- [62] D. Polley, M. Pancaldi, M. Hudl, P. Vavassori, S. Urazhdin and S. Bonetti, THz-driven demagnetization with perpendicular magnetic anisotropy: towards ultrafast ballistic switching, Phys. D: Appl. Phys. **51**, 084001 (2018).
- [63] M. Shalaby, A. Donges, K. Carva, R. Allenspach, P. M. Oppeneer, U. Nowak, and C. P. Hauri, Coherent and incoherent ultrafast magnetization dynamics in 3d ferromagnets driven by extreme terahertz fields, Phys. Rev. B **98**, 014405 (2018).
- [64] I. Razdolski, A. Alekhin, N. Ilin, J. P. Meyburg, V. Roddatis, D. Diesing, U. Bovensiepen, and A. Melnikov, Nanoscale interface confinement of ultrafast spin transfer torque driving non-uniform spin dynamics, Nat. Comm. **8**, 15007 (2017).
- [65] J. H. Yang, R. S. Craxton, and M. G. Haines, Explicit general solutions to relativistic electron dynamics in plane-wave electromagnetic fields and simulations of pondermotive acceleration, Plasma Phys. Control. Fusion **53**, 125006 (2011).
- [66] T. Henn, T. Kiessling, W. Ossau, L. W. Molenkamp, D. Reuter, and A. D. Wieck, Picosecond real-space imaging of electron spin diffusion in GaAs, Phys. Rev. B **88**, 195202 (2013)
- [67] C. Kittel, *Introduction to Solid State Physics*, 7th Ed., John Wiley & Sons, Inc., New York (1996).
- [68] C. von Korff Schmising, B. Pfau, M. Schneider, C. M. Günther, M. Giovannella, J. Perron, B. Vodungbo, L. Müller, F. Capotondi, E. Pedersoli, N. Mahne, J. Lüning, and S. Eisebitt, Imaging ultrafast demagnetization dynamics after a spatially localized optical excitation, Phys. Rev. Lett. **112**, 217203 (2014).
- [69] S. Ashok, C. Seibel, S. T. Weber, J. Brones and B. Rethfeld, Influence of diffusive transport on ultrafast magnetization dynamics, Appl. Phys. Lett. **120**, 142402 (2002).
- [70] J. Hurst, P.-A. Hervieux and G. Manfredi, Spin current generation by ultrafast laser pulses in ferromagnetic nickel films, Phys. Rev. B **97**, 014424 (2018).
- [71] S. Datta, *Quantum Transport: Atom to Transistor*, Cambridge University Press (2005).
- [72] G. P. Zhang and W. Hübner, Laser-induced ultrafast demagnetization in ferromagnetic metals, Phys. Rev. Lett. **85**, 3025 (2000).
- [73] G. P. Zhang, Y. H. Bai, T. Jenkins and T. F. George, Laser-induced ultrafast transport and



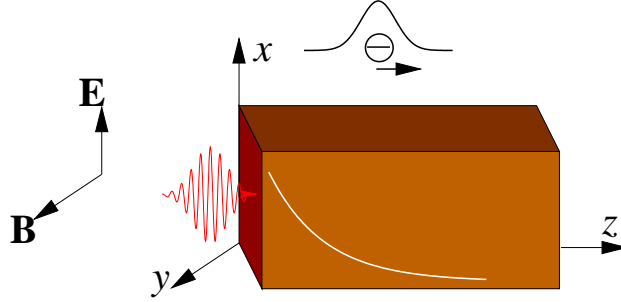


FIG. 1. A linearly polarized laser pulse propagating along the  $z$  axis with the electric field  $\mathbf{E}$  along the  $x$  axis and the magnetic field  $\mathbf{B}$  along the  $y$  axis. Inside the sample, both electric and magnetic fields reduce exponentially. The electron moves as a wavepacket along the  $z$  axis.

demagnetization at the earliest time: First-principles and real-time investigation, *J. Phys.: Condens. Matter* **30**, 465801 (2018).

[74] P. Földi, M. G. Benedict and V. S. Yakovlev, The effect of dynamical Bloch oscillations on optical-field-induced current in a wide-gap dielectric, *New J. Phys.* **15**, 063019 (2013).

[75] Y. Liu, U. Bierbrauer, C. Seick, S. T. Weber, Mo. Hofherr, N. Y. Schmidt, M. Albrecht, D. Steil, S. Mathias, H. C. Schneider, B. Rethfeld, B. Stadtmüller, and M. Aeschlimann, Ultrafast magnetization dynamics of Mn-doped L10 FePt with spatial inhomogeneity, *J. Magn. Magn. Mater.* **502**, 166477 (2020).

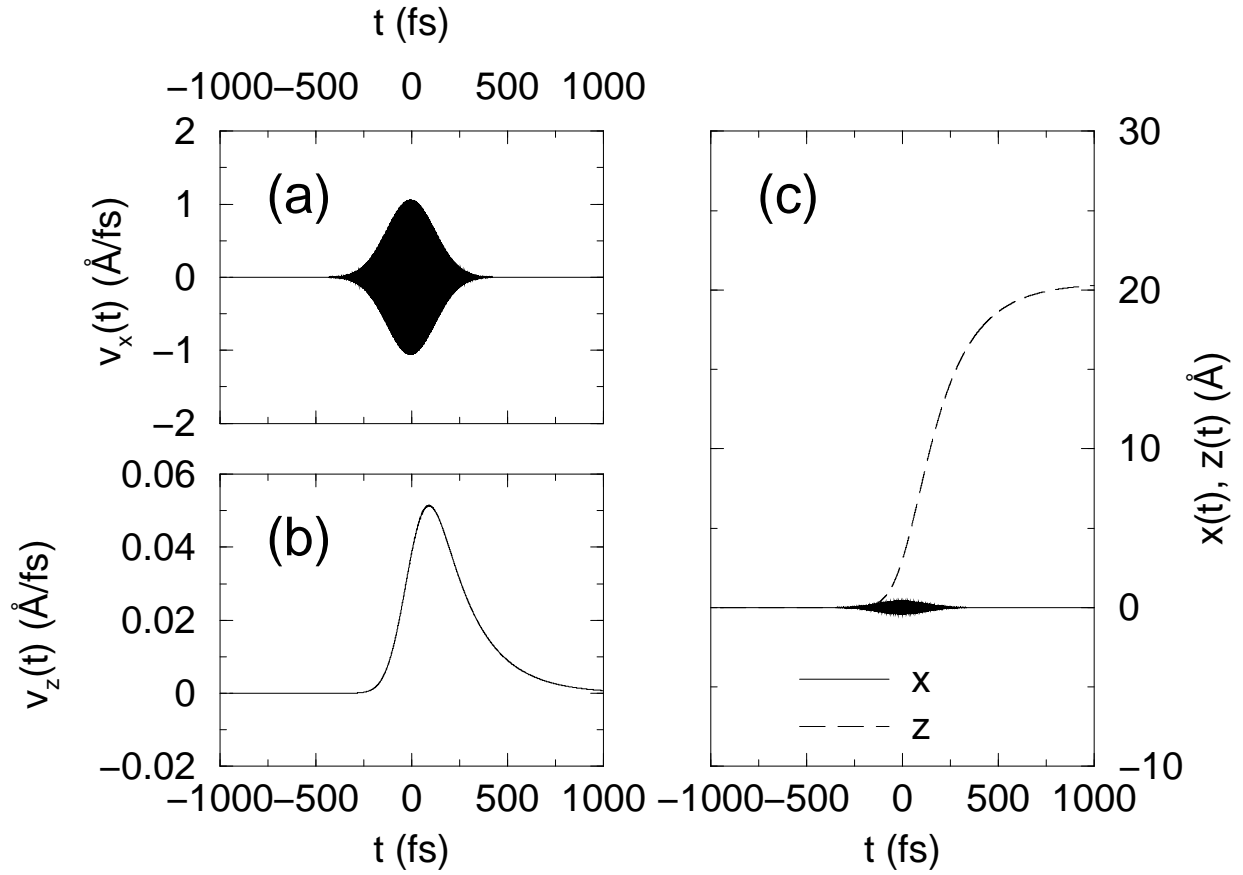


FIG. 2. (a) The electron velocity  $v_x$  strongly oscillates with time. Here we employ a pulse of  $\hbar\omega = 1.6$  eV,  $\tau = 180$  fs and  $A_0 = 0.15$  V/Å. (b)  $v_z$  does not have this oscillation. The peak around 100 fs is due to the damping  $\Gamma$ . (c) The electron moves little along the  $x$  axis (solid line) and it oscillates locally. But along the  $z$  axis, the electron clearly transports with a finite distance of about 20 Å (dashed line).

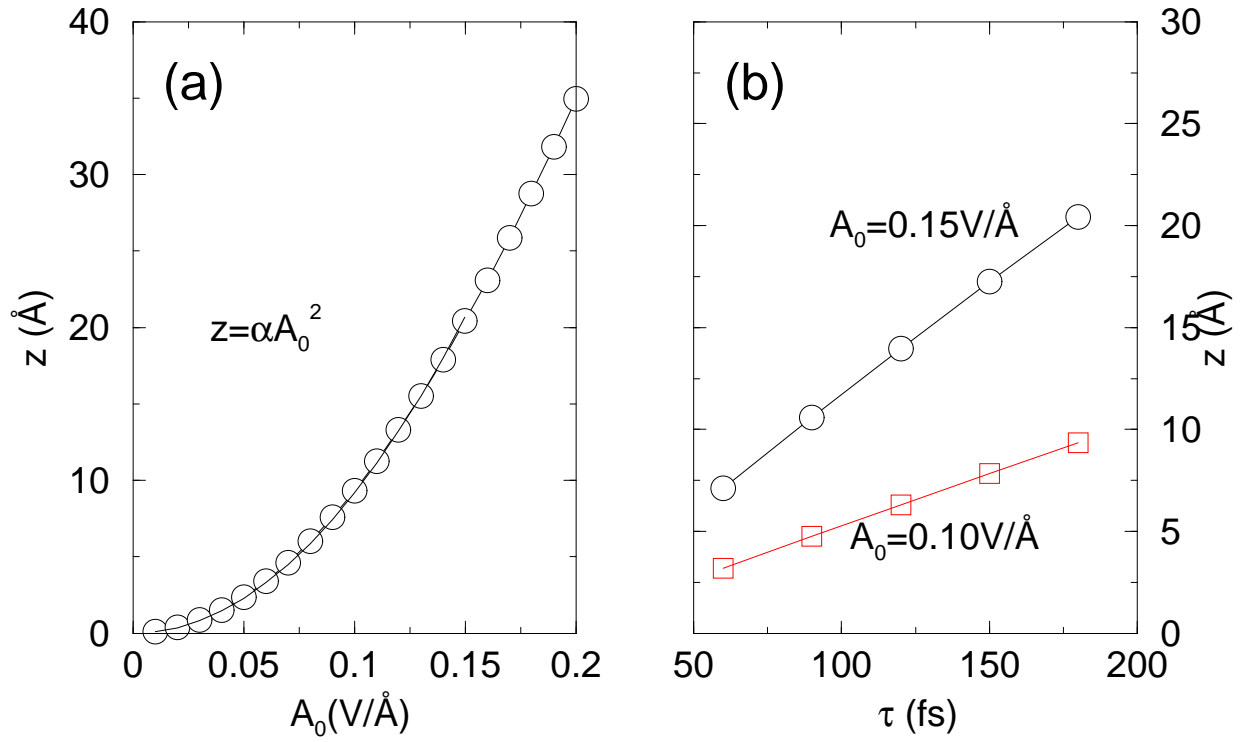


FIG. 3. (a) The electron final position  $z$  as a function of the laser amplitude  $A_0$  (circles). The line is a fit to the data up to  $A_0 = 0.15$  V/Å, where  $z = \alpha A_0^2$  and  $\alpha = 919.254 \text{ \AA}^3/\text{V}$ . Here  $\hbar\omega = 1.6$  eV and  $\tau = 180$  fs. (b)  $z$  as a function of  $\tau$  for a fixed  $\hbar\omega = 1.6$  eV for  $A_0 = 0.15$  V/Å (circles) and  $0.10$  V/Å (squares). (c)  $z$  as a function of  $\hbar\omega$ .

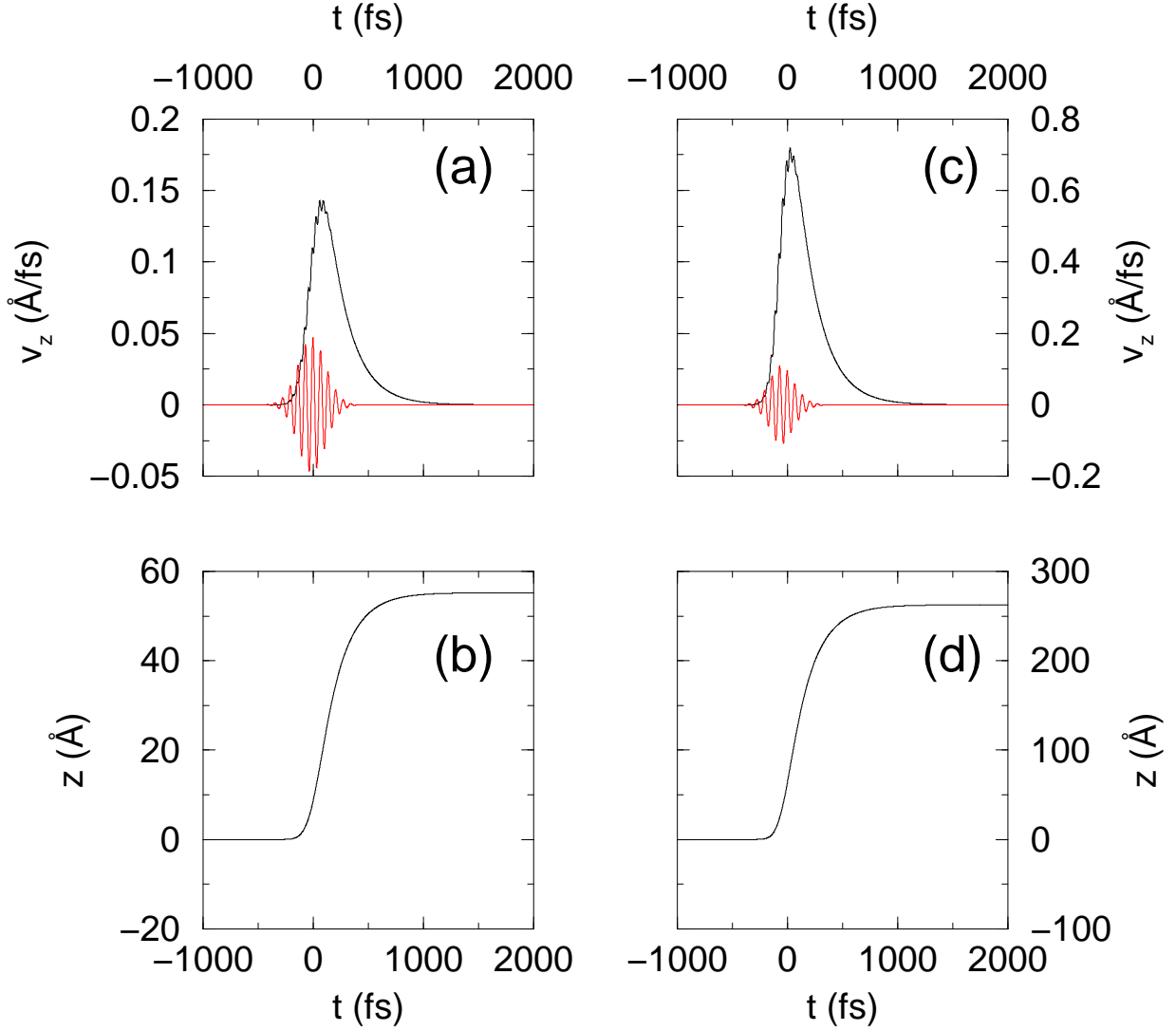


FIG. 4. (a)  $v_z$  as a function of time  $t$ . Our laser parameters are photon energy  $\hbar\omega = 0.06\text{eV}$ , duration  $\tau = 180 \text{ fs}$ , field amplitude  $A_0 = 0.05\text{V}/\text{Å}$ . Inset: our laser pulse. (b)  $z$  as a function of  $t$ .  $z$  reaches  $55.2 \text{ Å}$ . (c)  $v_z$  as a function of time  $t$  with  $A_0 = 0.15\text{V}/\text{Å}$ . (d) The dependence of  $z$  on  $t$ .  $z$  reaches  $262 \text{ Å}$ .

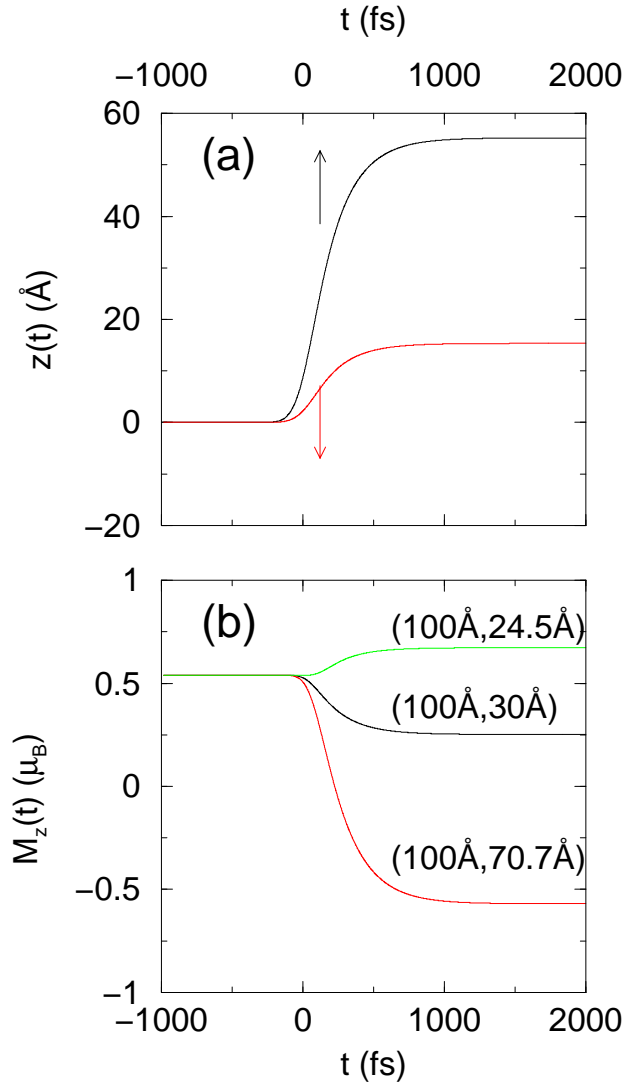


FIG. 5. (a)  $z$  for majority and minority spin channels as a function of time  $t$ , with  $\hbar\omega = 0.06$  eV, duration  $\tau = 180$  fs, field amplitude  $A_0 = 0.05\text{V}/\text{\AA}$ . The majority and minority spin channels are mimicked by the effective mass of the electron.  $m_{eff}^\uparrow = m_e$  and  $m_{eff}^\downarrow = 2m_e$ . (b) The spin moment changes as a function of time for three wavepackets whose widths are given on each curves.